Journal of Porous Media, 3(1), 31–44 (2000)

Vertical Free Convective Boundary-Layer Flow in a Porous Medium Using a Thermal Nonequilibrium Model

D. A. S. Rees[1] and I. Pop[2]

[1]Department of Mechanical Engineering, University of Bath, Bath BA2 7AY, UK and
[2]Faculty of Mathematics, University of Cluj, CP 253, Cluj R3400, Romania

ABSTRACT

In this article we study the effect of adopting a two-temperature model of microscopic heat transfer on the classical Cheng and Minkowycz (1977) vertical free convection boundary-layer flow in a porous medium. Such a model, which allows the solid and fluid phases not to be in local thermal equilibrium, is found to modify substantially the behavior of the flow relatively close to the leading edge, where the boundary layer is comprised of two distinct asymptotic regions. The numerical simulation of the developing boundary-layer relies heavily on near-leading-edge analysis to provide suitable boundary conditions. At increasing distances from the leading edge the difference between the temperatures of the fluid and solid phases decreases to zero, which corresponds to thermal equilibrium between the phases; this is confirmed by an asymptotic analysis.

Received July 17, 1998; Accepted August 20, 1998

NOMENCLATURE

a_0, b_0, a_1	constants
c	specific heat
g	gravity
h	solid/fluid heat transfer coefficient
p	fluid pressure
u	flux velocity in the x-direction
v	flux velocity in the y-direction
w	flux velocity in the z-direction
x	vertical distance from the leading edge
y	cross-stream coordinate
z	spanwise coordinate
F	outer-layer scaled stream function
H	scaled value of $\hat{h}$
K	permeability
R	Darcy–Rayleigh number
T	temperature

Greek symbols

β	coefficient of cubical expansion
ε	porosity
γ	a modified conductivity ratio
μ	fluid viscosity
λ	eigenvalue
θ	scaled temperature of fluid phase
Θ	outer-layer fluid temperature
ϕ	scaled temperature of solid phase
Φ	outer-layer solid temperature
ψ	stream function
ρ	fluid density
η	similarity variable
ζ	scaled similarity variable
ξ	scaled value of x

Other symbols, subscripts, and superscripts

-	dimensional
^	nondimensional
′	derivative with respect to η
f	fluid
s	solid
m	effective mean value
max	maximum value
w	wall
x	derivative with respect to x
y	derivative with respect to y
η	derivative with respect to η
ξ	derivative with respect to ξ
∞	ambient
0, 1, 2, . . .	terms in series expansion

INTRODUCTION

Buoyancy-driven convection in fluid-saturated porous media, originated from the empirical theory of Darcy [see the review by Lage (1998)] and supplemented by a suitable equation governing the transport of thermal energy, has been a popular area of research. This subject has received a considerable attention in the last three decades, partially owing to the increasing demand of our society for solutions to geophysical, environmental, and technological problems. Such problems are of interest, for example, in the utilization of geothermal energy, high-performance building insulation, regenerative heat exchangers, solar energy collectors, multishield structures used in the insulation of nuclear reactors, post-accident heat removal from nuclear reactor rubble beds, storage of agricultural products, pollutant dispersion in aquifers, sensible heat storage beds, enhanced recovery of petroleum resources, and in other applications. Continuous efforts have been devoted to the topic because of its practical importance, and considerable amount of information already exists. An extensive overview of the topic of buoyancy-induced flow in porous media has been documented in the book by Nield and Bejan (1992), and in the collection of 17 review articles edited by Ingham and Pop (1998).

The free convection boundary layer in a porous medium has been studied extensively for the past three decades since Wooding (1963) gave the first similarity solution for the flow produced by a point or line heat source. The case of convective flow from a vertical or a horizontal surface embedded in a porous medium is also a fundamentally interesting problem in heat transfer and has been studied intensively for more than two decades. Cheng and Chang (1976) and Cheng and Minkowycz (1977) developed, in a series of pioneering articles, a new class of boundary-layer problems in porous media. They demonstrated that a similarity solution exists for the steady free convection boundary-layer flow about vertical or horizontal flat plates

in a porous medium in which the wall temperature varies as a power of the distance from the leading edge of the plate. More detailed studies of these problems were given by Ingham and Brown (1986) and Merkin and Zhang (1990, 1992).

However, the usual way in which free convection boundary-layer flows are modeled is to assume that the convecting fluid and the porous medium are everywhere in local thermodynamic equilibrium. In this article we study in detail how vertical free convective boundary-layer flow is affected by the use of a nonequilibrium model of microscopic heat transfer between the fluid and the solid phase of the porous medium. The inclusion of more physical realism in the Darcian fluid model is important for the accurate modeling of any practical problem. A literature search indicates that this model of porous medium convection has been considered only a few times, two of the earliest of which are the studies of the Darcy–Bénard problem by Combarnous (1972) and Combarnous and Bories (1974). A recent restatement of the full equations are presented by Nield and Bejan (1992), where the equations governing the evolution of temperature in the solid and fluid phases are coupled by means of terms allowing the local transfer of heat to be proportional to the local temperature difference between the phases. Some articles pertinent to the two-energy equation model have been published for a Darcian or non-Darcian fluid flow through a packed bed. Reference may be made to the articles by Sözen and Vafai (1990), Sözen et al. (1991), Amiri and Vafai (1994), and Kuznetsov (1996a–c). The reviews by Kuznetsov (1998) and Vafai and Amiri (1998) give detailed information about the research on thermal nonequilibrium effects of fluid flow through a porous packed bed.

It is worth mentioning that a situation that displays some similarity to that treated here arises in what are usually termed conjugate convective flows, in which the heat is supplied to the convecting fluid through a bounding surface with a finite heat capacity. This results in the heat transfer rate through the surface being proportional to the local difference temperature with the ambient conditions (see, e.g., the recent review article by Kimura et al., 1997).

The plan in the present article is to determine the effect of adopting a two-temperature model of microscopic heat transfer on the classical Cheng and Minkowycz (1977) vertical free convection boundary-layer flow in a porous medium. The problem is formulated in the section that follows and it is shown that the governing boundary-layer equations are nonsimilar. It is further shown that this boundary-layer has a double layer structure near the leading edge and this situation is considered in detail in the third section. The numerical solution of the full boundary-layer equations is given in the fourth section. It is shown, in particular, how it is possible to incorporate the outer-layer behavior into the Keller-box procedure. Asymptotic solutions far from the leading edge are considered in the fifth section, where it is found that an eigensolution of arbitrary amplitude appears quite early in the asymptotic expansion, thereby limiting the applicability of the analysis. The results are discussed in the sixth section, with particular reference to the rate of heat transfer.

MATHEMATICAL FORMULATION

The equations governing Darcy–Boussinesq convection in a saturated porous medium are usually studied by first invoking the assumption that the solid and fluid phases of the medium are in local thermal equilibrium. In this article we study one particular case where a two-temperature model of microscopic heat transfer applies. The governing equations are

$$\bar{u}_{\bar{x}} + \bar{v}_{\bar{y}} + \bar{w}_{\bar{z}} = 0 \tag{1a}$$

$$\bar{u} = -\frac{K}{\mu}\frac{\partial \bar{p}}{\partial \bar{x}} - \frac{\rho_f g \beta K}{\mu}(T_f - T_\infty), \tag{1b,c,d}$$

$$\bar{v} = -\frac{K}{\mu}\frac{\partial \bar{p}}{\partial \bar{y}}, \qquad \bar{w} = -\frac{K}{\mu}\frac{\partial \bar{p}}{\partial \bar{z}}$$

$$\varepsilon(\rho c)_f \frac{\partial T_f}{\partial t} + (\rho c)_f \bar{u}\cdot\nabla T_f = \varepsilon k_f \nabla^2 T_f + h(T_s - T_f) \tag{1e}$$

$$(1-\varepsilon)(\rho c)_s \frac{\partial T_s}{\partial t} = (1-\varepsilon)k_s \nabla^2 T_s - h(T_s - T_f) \tag{1f}$$

(see Nield and Bejan (1992)). Here, $\bar{u}$, $\bar{v}$, and $\bar{w}$ are the fluid flux velocities in the streamwise (upwards), cross-stream, and spanwise directions, $\bar{x}$, $\bar{y}$, and $\bar{z}$, respectively, and t is the time. The pressure is $\bar{p}$ and the temperature is T, where the f and s subscripts denote the fluid and solid phases, respectively. The following are the other fluid and medium properties: K is the permeability, μ the fluid viscosity, ρ the density, c the specific heat, β the coefficient of cubical expansion, ε the porosity, and k the thermal conductivity. In Eqs. (1e) and (1f) h is a coefficient that is used to model the microscopic transfer of heat between the fluid and solid phases.

In this article we consider the steady two-dimensional flow which is induced by a vertical heated surface held at the constant temperature, T_w, and embedded in a porous medium with ambient temperature, T_∞, where $T_w > T_\infty$. Here we assume that the flow is steady and two-dimensional for

the results of the studies of Rees (1993), Lewis et al. (1995), and Storesletten and Rees (1998) indicate that the steady, two-dimensional vertical boundary layer flow from a constant temperature surface is stable when there is local thermal equilibrium. A very recent numerical simulation of the unsteady elliptic version of the present boundary-layer problem suggests that the absence of local equilibrium does not destabilize the flow, at least to two-dimensional disturbances; see Rees (1998a). Therefore the flow may safely be assumed to be two-dimensional, and we shall consider the final steady-state convection. Therefore we can set $\bar{w} = 0$ and neglect all t and $\bar{z}$ derivatives in Eq. (1). After this simplification, Eqs. (1a–f) may now be nondimensionalized using the following transformations:

$$(\bar{x}, \bar{y}) = d(\hat{x}, \hat{y}), \qquad (\bar{u}, \bar{v}) = \frac{\varepsilon k_f}{(\rho c)_f d}(\hat{u}, \hat{v}), \tag{2a,b,c}$$

$$\bar{p} = \frac{k_f \mu}{(\rho c)_f K}\hat{p}$$

$$T_f = (T_w - T_\infty)\theta + T_\infty, \qquad T_s = (T_w - T_\infty)\phi + T_\infty \tag{2d,e}$$

where d is a suitably defined macroscopic lengthscale. A further simplification is afforded by the introduction of a streamfunction, $\hat{\psi}$, according to $\hat{u} = \hat{\psi}_{\hat{y}}$ and $\hat{v} = -\hat{\psi}_{\hat{x}}$. Equations (1a–f) now become

$$\nabla^2\hat{\psi} = R\frac{\partial\theta}{\partial\hat{y}} \tag{3a}$$

$$\nabla^2\theta = \hat{h}(\theta - \phi) + \frac{\partial\hat{\psi}}{\partial\hat{y}}\frac{\partial\theta}{\partial\hat{x}} - \frac{\partial\hat{\psi}}{\partial\hat{x}}\frac{\partial\theta}{\partial\hat{y}} \tag{3b}$$

$$\nabla^2\phi = \hat{h}\gamma(\phi - \theta) \tag{3c}$$

where

$$\hat{h} = hd^2/\varepsilon k_f \quad \text{and} \quad \gamma = \frac{\varepsilon k_f}{(1-\varepsilon)k_s} \tag{3d,e}$$

are dimensionless constants, and

$$R = \frac{\rho_f(\rho c)_f g\beta(T_w - T_\infty)Kd}{\varepsilon\mu k_f} \tag{3f}$$

is a Darcy–Rayleigh number based on the fluid properties. In particular, the Rayleigh number is based on k_f, the conductivity of the fluid, rather than

$$k_m = \varepsilon k_f + (1-\varepsilon)k_s \tag{3g}$$

which is generally taken to be the effective conductivity of the saturated porous medium. The value γ is a porosity-scaled conductivity ratio, and we will be considering values in the range from 10^{-5} to 10^{-1}, which covers most practical applications. Low values of γ generally correspond to a relatively poorly conducting fluid such an air in a metallic porous medium.

Next we introduce the usual boundary layer scalings (Rees, 1998b):

$$\hat{x} = x, \qquad \hat{y} = R^{-1/2}y, \qquad \hat{\psi} = R^{1/2}\psi \tag{4a,b,c}$$

into Eqs. (3a–g) to obtain

$$\frac{\partial^2\psi}{\partial y^2} = \frac{\partial\theta}{\partial y} \tag{5a}$$

$$\frac{\partial^2\theta}{\partial y^2} = H(\theta - \phi) + \frac{\partial\psi}{\partial y}\frac{\partial\theta}{\partial x} - \frac{\partial\psi}{\partial x}\frac{\partial\theta}{\partial y} \tag{5b}$$

$$\frac{\partial^2\phi}{\partial y^2} = H\gamma(\phi - \theta) \tag{5c}$$

where we have omitted terms that are asymptotically small compared with the retained terms as $R \to \infty$. In Eq. (5a–c) H is defined according to

$$\hat{h} = RH \tag{6}$$

such a scaling for $\hat{h}$, where $H = O(1)$ as $R \to \infty$, allows the detailed study of how the boundary-layer undergoes the transition from strong thermal nonequilibrium near the leading edge to thermal equilibrium (at least to leading order) far from the leading edge. However, if it is insisted that $\hat{h} = O(1)$ as $R \to \infty$, then the analysis of the rest of the article is unaffected if Eqs. (4a–c) are replaced by $\hat{x} = Rx$, $\hat{y} = y$, and $\hat{\psi} = R\psi$—the implication of these alternative transformations is that the transition from strong nonequilibrium to equilibrium takes place at increasing distances from the leading edge as $\hat{h}$ decreases (i.e., as the local rate of heat transfer between the phases decreases in strength). The boundary conditions are

$$\psi = 0, \qquad \theta = 1, \qquad \phi = 1 \quad \text{at} \quad y = 0 \qquad \text{and}$$

$$\frac{\partial\psi}{\partial y}, \theta, \phi \to 0 \quad \text{as} \quad y \to \infty \tag{7}$$

These boundary conditions allow Eq. (5a) to be integrated once to yield

$$\frac{\partial\psi}{\partial y} = \theta \tag{8}$$

The usual boundary-layer transformation for vertical free convection of a Darcy fluid from a uniform temperature surface may now be introduced (Cheng and Minkowycz, 1977):

$$\psi = x^{1/2} f(x, \eta), \qquad \theta = \theta(x, \eta), \qquad \phi = \phi(x, \eta) \tag{9a,b,c}$$

where

$$\eta = \frac{y}{x^{1/2}} \tag{10}$$

and where f, θ, and ψ satisfy

$$f' = \theta,$$

$$\theta'' + \frac{1}{2} f\theta' = Hx(\theta - \phi) + x(f'\theta_x - \theta' f_x), \tag{11a,b,c}$$

$$\phi'' = H\gamma x(\phi - \theta)$$

subject to the boundary conditions,

$$f = 0, \quad \theta = 1, \quad \phi = 1 \quad \text{at} \quad \eta = 0, \quad \text{and} \quad \theta, \phi \to 0 \quad \text{as} \quad \eta \to \infty \tag{11d}$$

In Eq. (11a–c) primes denote derivatives with respect to η, and the x-subscript denotes derivatives with respect to x. Finally we note that H may be scaled out of Eqs. (11a–c) using $\tilde{x} = Hx$. However, the analysis of the next section is presented more easily if Eqs. (11a–c) are kept as they are.

ASYMPTOTIC ANALYSIS NEAR THE LEADING EDGE

Equations (11a–d) form a system of parabolic equations whose solution is nonsimilar due to the x-dependent forcing induced by the terms proportional to H. Normally such a nonsimilar set of equations is solved using a marching scheme, such as the Keller-box method (Cebeci and Bradford, 1984). Beginning at the leading edge, where the system reduces to an ordinary differential system, the solution at each streamwise station is obtained in turn at increasing distances from the leading edge. Again, such solutions are typically supplemented by a series expansion for small values of x, and by an asymptotic analysis for large values of x; the former often reveals no further information except perhaps validating the numerical scheme, but the latter can often yield insights that may not be immediately obvious from the numerical solution.

The present problem is not of this general nature, however, for when $x = 0$ the equation for ϕ, (11c), cannot be solved with both boundary conditions satisfied. Immediately this suggests that the solution for ϕ may be obtained more readily in terms of its y-variation using Eq. (5c). Thus this boundary layer has the rather unusual property of having a double-layer structure near the leading edge, rather than far from it as is often the case (see Rees and Pop, 1994, Rees and Bassom, 1996; Rees, 1997). This complicates considerably the numerical simulation of the flow because it is now essential to derive the near-leading-edge solution carefully before embarking on the numerical work.

The small-x analysis is facilitated by setting

$$\psi = x^{1/2} F(x, y), \quad \theta = \Theta(x, y), \quad \phi = \Phi(x, y) \tag{12a,b,c}$$

in Eqs. (5a–c), which become

$$x^{1/2} F_y = \Theta, \qquad x^{1/2}\Theta_{yy} + \frac{1}{2} F\Theta_y = Hx^{1/2}(\Theta - \Phi) + x(F_y\Theta_x - \Theta_y F_x), \qquad \Phi_{yy} = H\gamma(\Phi - \Theta) \tag{13a,b,c}$$

Near the leading edge we will solve Eqs. (11a–d) and (13a–c) using the method of matched asymptotic expansions with asymptotic matching between the two regimes (which are $\eta = O(1)$ and $y = O(1)$ as $x \to 0$) and subject to the boundary conditions

$$f = 0, \quad \theta = 1, \quad \phi = 1 \quad \text{at} \quad \eta = 0, \quad \text{and} \quad \Theta, \Phi \to 0 \quad \text{as} \quad y \to \infty \tag{14}$$

The solutions of Eqs. (11a–d) and (13a–c) may be found by assuming the following power series expansion in terms of $x^{1/2}$: let

$$f(x, \eta) = f_0(\eta) + x^{1/2} f_1(\eta) + x f_2(\eta) + \cdots \tag{15}$$

$$F(x, y) = F_0(y) + x^{1/2} F_1(y) + x F_2(y) + \cdots \tag{16}$$

with corresponding expressions for θ, ϕ, Θ, and Φ. When $\eta = O(1)$ as $x \to 0$ we obtain the main boundary layer which will be termed the inner layer. The relatively thick region where $y = O(1)$ will be termed the outer layer.

At $O(1)$ in the inner layer we obtain the equations

$$f_0' = \theta_0, \qquad \theta_0'' + \frac{1}{2} f_0 \theta_0' = 0, \qquad \phi_0'' = 0 \tag{17a,b,c}$$

The solution for f_0 and θ_0 is well known and was first presented in Cheng and Minkowycz (1977). The main features of this solution that are of interest here are that

$$f_0 \to 1.61613 \equiv a_0 \quad \text{as} \quad \eta \to \infty \quad \text{and} \quad \theta_0'(0) = -0.443748 \equiv b_0 \tag{18a,b}$$

In addition θ_0 becomes exponentially small as $\eta \to \infty$. The solution for ϕ_0 is

$$\phi_0 = 1 \tag{19}$$

These results suggest that there is an outer solution for F_0, that Θ_0 is very likely to be zero, and that the matching condition for Φ_0 at $y = 0$ is $\Phi(0) = 1$.

At $O(1)$ in the outer layer we obtain the equation

$$\frac{d^2\Phi_0}{dy^2} = H\gamma\Phi_0 \tag{20}$$

where we have assumed that $\Theta_0 = 0$. The solution of Eq. (20) subject to the matching condition at $y = 0$ is

$$\Phi_0 = e^{-\sqrt{H\gamma}y} \tag{21}$$

In turn, Eq. (21) provides the matching condition for ϕ as $\eta \to \infty$: as

$$\Phi = 1 - \sqrt{H\gamma}y + \cdots, \quad \text{for small } y \tag{22a}$$

then the replacement of y by $x^{1/2}\eta$ and the setting of $x \to 0$ will yield

$$\phi = 1 - (\sqrt{H\gamma}\eta)x^{1/2} + \cdots \quad \text{as } \eta \to \infty \tag{22b}$$

Thus the matching condition for ϕ_1 is that $\phi_1 \sim -\sqrt{H\gamma}\eta$ as $\eta \to \infty$.

At $O(x^{1/2})$ in the inner layer we have

$$f_1' = \theta_1, \quad \theta_1'' + \frac{1}{2}(f_0\theta_0' + 2f_1\theta_0' - f_0'\theta_1) = 0,$$
$$\phi_1'' = 0 \tag{23a,b,c}$$

subject to the conditions

$$f_1 = 0, \quad \theta_1 = 0, \quad \phi_1 = 0 \quad \text{at} \quad \eta = 0,$$
$$\text{and} \quad \phi_1 \sim -\sqrt{H\gamma}\eta \quad \text{as} \quad \eta \to \infty \tag{24}$$

Normally one would also specify the condition that $\theta_1 \to 0$ as $\eta \to \infty$, but the insistence that this is the case here leads to an inconsistency at the next order in the asymptotic analysis. The form of the equation for θ_1 is such that it is possible for θ to tend toward a constant value when $\eta \to \infty$, and this leads to a consistent analysis involving a nonzero fluid temperature in the outer layer. Thus the relatively strong solid temperature ($O(1)$) induces a relatively weak fluid temperature ($O(x^{1/2})$) in the outer layer. As Eq. (23b) is linear, it may be solved using the boundary condition $\theta_1'(0) = 1$ and the resulting solution rescaled when an appropriate matching condition is found from the $O(x^{1/2})$ outer-layer solution, below. With this boundary condition we find that $\theta_1 \to 7.06066$ as $\eta \to \infty$. A graph of θ_1 subject to this boundary condition is shown in Fig. 1. The solution for ϕ_1 is, simply,

$$\phi_1 = -\sqrt{H\gamma}\eta \tag{25}$$

and therefore the variation of ϕ within the inner layer is passive this far in the analysis, and is given by the Taylor

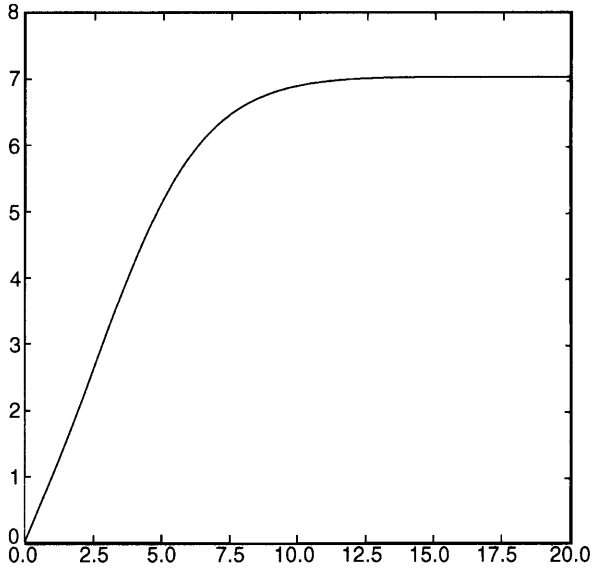

Figure 1. $\theta_1(\eta)$ as obtained from solving Eqs. (23a, b) using the boundary conditions, $\theta_1(0) = 0$, $\theta_1'(0) = 1$ and $\theta_1' \to 0$ as $\eta \to \infty$.

series expansion of the leading-order outer-layer solution [Eq. (21)].

At $O(x^{1/2})$ in the outer layer the equations are

$$\frac{dF_0}{dy} = \Theta_1, \qquad F_0\frac{d\Theta_1}{dy} - \Theta_1\frac{dF_0}{dy} = -2H\Phi_0,$$
$$\frac{d\Phi_1}{dy} = H\gamma(\Phi_1 - \Theta_1) \tag{26a,b,c}$$

Substitution of Eqs. (26a) and (21) into (26b) yields

$$F_0\frac{d^2F_0}{dy^2} - \frac{dF_0}{dy}\frac{dF_0}{dy} = -2He^{-\sqrt{H\gamma}y} \tag{27}$$

for which there exists two solutions in the form $F_0 = A + Be^{-\sqrt{H\gamma}y}$ where A and B are constants. Only one of these solutions yields positive values for Θ_1 using Eq. (26a), and therefore we obtain:

$$F_0 = \left(\frac{a_0 + \sqrt{a_0^2 + 8/\gamma}}{2}\right) + \left(\frac{a_0 + \sqrt{a_0^2 + 8/\gamma}}{2}\right) \tag{28a}$$

$$\Theta_1 = -\sqrt{H\gamma}\left(\frac{a_0 - \sqrt{a_0^2 + 8/\gamma}}{2}\right)e^{-\sqrt{H\gamma}y} \tag{28b}$$

and

$$\Phi_1 = -H\gamma\left(\frac{a_0 - \sqrt{a_0^2 + 8/\gamma}}{2}\right)ye^{-\sqrt{H\gamma}y} \tag{28c}$$

where a_0 is given in Eq. (15a). If, in Eqs. (23a–c), we allow $\theta_1 \to a_1$ as $\eta \to \infty$, then asymptotic matching with Eq. (28b) gives a_1 as

$$a_1 = -\sqrt{H\gamma}\left(\frac{a_0 - \sqrt{a_0^2 + 8/\gamma}}{2}\right) \tag{29}$$

and therefore

$$\theta_1'(0) = a_1/7.06066 \tag{30}$$

We conclude that the temperature field near the leading edge has a two-layer structure, with the temperature profile of the solid phase appearing strongly in the outer layer for asymptotically small values of x. The fluid temperature profile appears only at $O(x^{1/2})$ in the outer layer, being confined mainly within the inner layer. The rates of heat transfer for the two phases are given by

$$\frac{\partial\theta}{\partial\eta}\Big|_{\eta=0} \sim b_0 + \frac{a_1}{7.06066}x^{1/2} \tag{31a}$$

$$\frac{\partial\phi}{\partial\eta}\Big|_{\eta=0} \sim -\sqrt{H\gamma}\,x^{1/2} \tag{31b}$$

as $x \to 0$. These asymptotic forms are confirmed to three or four significant figures (depending on the value of γ) by the detailed numerical solutions described in the next section.

NUMERICAL SOLUTION

In this section we describe in detail how Eqs. (11a–d) are solved numerically and, in particular, how it is possible to incorporate the outer-layer behavior into the solution procedure. But first it is essential to rescale the x coordinate. Given the form of the surface rates of heat transfer given in Eq. (31) we see that these values rise infinitely fast as x increases from zero; this would cause substantial inaccuracies in the numerical solution. Therefore we set

$$\xi = x^{1/2} \tag{32}$$

in Eqs. (11a–d) to get

$$f' = \theta, \qquad \theta'' + \frac{1}{2}f\theta' = H\xi^2(\theta - \phi)$$
$$+\frac{1}{2}\xi(f'\theta_\xi - \theta' f_\xi), \qquad \phi'' = H\gamma\xi^2(\phi - \theta) \tag{33a,b,c}$$

In the last section we saw that the leading-order solutions in the outer layer, Φ_0 and Θ_1, are both proportional to $e^{-\sqrt{H\gamma}y}$. When rewritten in terms of the inner-layer coordinate, η, this term becomes $e^{-\sqrt{H\gamma}\xi\eta}$. It decays with an e-folding distance of $(H\gamma)^{-1/2}\xi^{-1}$. This should be compared with the e-folding distance of the inner layer solution at the leading edge, $2/a_0$, which is obtained by noting that θ_0 is asymptotically proportional to $e^{-a_0\eta/2}$ for large values of η. Therefore we need to incorporate the very slow decay corresponding to the outer-layer solution by modifying the boundary conditions for both θ and ϕ. We note that the decay becomes quicker as ξ increases, and therefore, when the maximum value of η, η_{max}, is sufficiently large, the outer-layer behavior is readily accounted for.

Our numerical strategy is as follows. When $\xi = 0$ Eqs. (33a–c) are solved subject to the boundary conditions:

$$\begin{aligned} &\eta = 0: \quad f = 0, \quad \theta = 1, \quad \phi = 1, \\ &\eta = \eta_{max}: \quad \theta = 0, \quad \phi = 1 \end{aligned} \tag{34}$$

where, of course, the Cheng and Minkowycz (1977) solution is obtained for f and θ with $\phi = 1$. For $\xi > 0$ the boundary conditions are

$$\begin{aligned} &\eta = 0: \quad f = 0, \quad \theta = 1, \quad \phi = 1, \\ &\eta = \eta_{max}: \quad \frac{\partial\theta}{\partial\eta} + \sqrt{H\gamma}\xi\theta = 0, \quad \frac{\partial\phi}{\partial\eta} + \sqrt{H\gamma}\xi\phi = 0 \end{aligned} \tag{35}$$

Both the boundary conditions at $\eta = \eta_{max}$ force the required exponential decay, so that the values of θ and ϕ at η_{max} are not necessarily small. However, we must choose η_{max} to be sufficiently large that both θ and ϕ at η_{max} become small before ξ increases to such an extent that higher order solutions contaminate the leading-order decay rate. When ξ is such that both θ and ϕ at η_{max} are $<10^{-6}$ then the boundary conditions are changed to

$$\begin{aligned} &\eta = 0: \quad f = 0, \quad \theta = 1, \quad \phi = 1, \\ &\eta = \eta_{max}: \quad \theta = 0, \quad \phi = 0 \end{aligned} \tag{36}$$

Equations (33a–c) were solved using the Keller-box method which is described in Cebeci and Bradshaw (1984). Typically the governing equations are reduced to first-order form in terms of η and are then discretized using central differences in both the ξ and η directions. The solution at each streamwise station is then obtained using a multidimensional Newton–Raphson iteration scheme. For the present problem such an implementation was found to cause very large pointwise oscillations in the ξ-direction that could not be reduced to a satisfactory level by grid refinement; such a phenomenon may be explained by appealing to the similarity between the Keller-box method and the Crank-Nicholson method. Therefore we modified the methodology by using backward differences in the ξ-direction, a device that, although formally less accurate, has the advantage of much better stability properties. This

technique has recently been used very successfully, and for the same reason, by Rees (1998b), who considered vertical free convection in a layered porous medium.

Nonuniform grids of both the ξ and η values were used. The η-values ranged between 0 and 2000; the grid was concentrated toward $\eta = 0$, but the details of the precise distribution are not important if the resolution is good. The ξ-values were chosen by insisting that the intervals followed a geometric progression. We used 421 points between $\xi = 0$ and $\xi = 100$ where the first interval was $<10^{-6}$. Grid resolution tests for all values of γ studied showed that four significant figures of accuracy were maintained in all cases.

The basic implementation of Cebeci and Bradshaw (1984) was modified further by the inclusion of a numerical differentiation routine to compute the Jacobian matrix used in the Newton–Raphson iteration scheme. This technique has been used successfully in other numerical simulations [see Rees (1997) and Rees (1998b)]. Such a facility allows a very much more rapid code development, although the execution time is greater than when the Jacobian is specified explicitly by the programmer.

In the numerical solution we have set $H = 1$; solutions for other values of H are obtained by a simple rescaling of x, as discussed earlier. Consequently we are left with a one-parameter family of solutions characterized by different values of γ.

SOLUTION FAR FROM THE LEADING EDGE

The form of the terms involving Hx in Eqs. (11a–c) would seem to suggest that these terms will dominate their respective equations when x is asymptotically large. One possible means of balancing this large magnitude is to insist that the θ'' and ϕ'' terms are correspondingly large, thereby implying that there is a thin sublayer embedded within the inner layer. Such is the case in similar studies carried out by Rees and Pop (1994), Rees and Bassom (1996), and Rees (1997). However, the numerical evidence indicates that θ and ϕ become almost identical as ξ increases, and therefore it is quite possible that the difference between θ and ϕ is $O(x^{-1})$ for large x, with no thin sublayer. We can make ϕ the subject of the equation by repeated substitution of Eq. (11c) into itself:

$$\phi = \theta + (H\gamma x)^{-1}\theta'' + (H\gamma x)^{-2}\theta'''' + (H\gamma x)^{-3}\theta'''''' + \cdots \tag{37}$$

Substitution of Eq. (37) into (11b) gives

$$\left(1+\frac{1}{\gamma}\right)\theta'' + \frac{1}{2}f\theta' = x(f'\theta_x - \theta' f_x) - \gamma^{-1}[(H\gamma x)^{-1}\theta'''' + (H\gamma x)^{-2}\theta'''''' + \cdots] \tag{38}$$

A straightforward solution of Eq. (38) in the form of an inverse power series in x leads to an insoluble system of equations at $O(x^{-1})$. This arises because the homogeneous form of that system admits an eigensolution of arbitrary amplitude. Therefore we introduce a logarithmic term at the appropriate place and expand f and θ in the series

$$(f, \theta) = (f^{(0)}, \theta^{(0)}) + x^{-1}\ln x(f^{(1L)}, \theta^{(1L)}) + x^{-1}(f^{(1)}, \theta^{(1)}) + \cdots \tag{39}$$

Substitution into Eq. (11a) and (38) yields

$$f_\eta^{(0)} = \theta^{(0)}, \qquad \left(1+\frac{1}{\gamma}\right)\theta_{\eta\eta}^{(0)} + \frac{1}{2}f^{(0)}\theta_\eta^{(0)} = 0 \tag{40a,b}$$

$$f_\eta^{(1L)} = \theta^{(1L)}, \qquad \left(1+\frac{1}{\gamma}\right)\theta_{\eta\eta}^{(1L)} + \frac{1}{2}[f^{(0)}\theta_\eta^{(1L)} + 2f_\eta^{(0)}\theta^{(1L)} - f^{(1L)}\theta_\eta^{(0)}] = 0 \tag{41a,b}$$

$$f_\eta^{(1)} = \theta^{(1)}, \qquad \left(1+\frac{1}{\gamma}\right)\theta_{\eta\eta}^{(1)} + \frac{1}{2}[f^{(0)}\theta_\eta^{(1)} + 2f_\eta^{(0)}\theta^{(1)} - f^{(1)}\theta_\eta^{(0)}] = -H^{-1}\gamma^{-2}\theta_{\eta\eta\eta\eta}^{(0)} + f_\eta^{(0)}\theta^{(1L)} - \theta_\eta^{(0)}f^{(1L)} \tag{42a,b}$$

subject to

$$\eta = 0: \quad f^{(0)} = 0, \quad \theta^{(0)} = 1, \quad f^{(1L)} = 0, \quad \theta^{(1L)} = 0, \quad f^{(1)} = 0, \quad \theta^{(1)} = 0 \tag{43a}$$

$$\eta \to \infty: \quad \theta^{(0)}, \theta^{(1L)}, \theta^{(1)} \to 0 \tag{43b}$$

Equations (40a, b) may be reduced to exactly the same form as (14a, b) using the substitution

$$\zeta = \left(1+\frac{1}{\gamma}\right)^{-1/2}\eta, \qquad f = \left(1+\frac{1}{\gamma}\right)^{-1/2}\tilde{f} \tag{44a,b}$$

Therefore Eqs. (40), (41), and (42) reduce to

$$\tilde{f}_\zeta^{(0)} = \theta^{(0)}, \qquad \theta_{\zeta\zeta}^{(0)} + \frac{1}{2}\tilde{f}^{(0)}\theta_\zeta^{(0)} = 0 \tag{45a,b}$$

$$\tilde{f}_\zeta^{(1L)} = \theta^{(1L)}, \qquad \theta_{\zeta\zeta}^{(1L)} + \frac{1}{2}[\tilde{f}^{(0)}\theta_\zeta^{(1L)} + 2\tilde{f}_\zeta^{(0)}\theta^{(1L)} - \tilde{f}^{(1L)}\theta_\zeta^{(0)}] = 0 \tag{46a,b}$$

$$\tilde{f}_\zeta^{(1)} = \theta^{(1)}, \qquad \theta_{\zeta\zeta}^{(1)} + \frac{1}{2}[\tilde{f}^{(0)}\theta_\zeta^{(1)} + 2\tilde{f}_\zeta^{(0)}\theta^{(1)} - \tilde{f}^{(1)}\theta_\zeta^{(0)}]$$
$$= -H^{-1}(1+\gamma)^{-2}\theta_{\zeta\zeta\zeta\zeta}^{(0)} + \tilde{f}_\zeta^{(0)}\theta^{(1L)} - \theta_\zeta^{(0)}\tilde{f}^{(1L)} \quad (47a,b)$$

The solution of Eq. (46a, b) is

$$\tilde{f}^{(1L)} = \lambda(\zeta\tilde{f}_\zeta^{(0)} - \tilde{f}^{(0)}), \qquad \theta^{(1L)} = \lambda\zeta\theta_\zeta^{(0)} \quad (48)$$

See Daniels and Simpkins (1984), where λ is a constant whose value may be found by insisting that Eqs. (47a, b) have a solution. As Eqs. (47a, b) also admit a solution of the form (48), it is necessary to supply one extra boundary condition in order to "normalize" the solution and yield a value for λ. Therefore we set $\theta^{(1)}(0) = 0$, although any other choice would yield the same value for λ. The solutions of Eqs. (45a, b) and (47 a, b) were obtained using a standard fourth-order Runge-Kutta scheme with an associated shooting method facility and we obtain

$$\theta_\zeta^{(0)}(\zeta = 0) = b_0 = -0.443748, \qquad \lambda = -0.0984563,$$
$$\theta_\zeta^{(1L)}(\zeta = 0) = \lambda b_0 \quad (49a,b,c)$$

In terms of η, the fluid rate of heat transfer is

$$\frac{\partial\theta}{\partial\eta}\Big|_{\eta=0} = \left(1 + \frac{1}{\gamma}\right)^{-1/2}[b_0 + \lambda b_0 x^{-1}\ln x + O(x^{-1})] \quad (50)$$

Using Eq. (37) the solid rate of heat transfer at $\eta = 0$ is identical to the fluid rate, the leading-order difference lying at $O(x^{-1})$. We note that the numerical solution confirms the value of $x(\phi' - \theta')$ at $\eta = 0$ to four significant figures at $\xi = 50$ ($x = 2500$).

RESULTS AND CONCLUSION

The numerical method described in the fourth section was used to solve Eqs. (11a–d) for various values of γ. The solutions obtained are summarized in Figs. 2 and 3. We note, for the sake of completeness, that the asymptotic predictions for both small and large values of x(or ξ) are confirmed to a high degree by the numerical solution.

Figure 2 displays the isotherms for the two phases in a Cartesian coordinate system, and seven different values for γ are presented there. It is important to note that the y-coordinate has been stretched considerably [see Eq. (4b)] and the boundary layer is very thin, despite the appearance of Fig. 2. It is very clear from the isotherm plots that a state of local thermal equilibrium, indicated by the isotherms for the two phases being virtually coincident, is reached relatively close to the leading edge when γ is large. Conversely, when γ is relatively small, thermal equilibrium is reached at relatively large distances from the leading edge. A large value of γ corresponds to the fluid having a high thermal conductivity relative to the solid, thereby allowing the fluid properties to dominate the development of the boundary-layer flow. This is also confirmed by the fact that the e-folding distance of the outer-layer solid phase temperature profile becomes smaller as γ increases; see Eq. (21). Further, the thickness of the boundary-layer at large distances from the leading edge is proportional to $(1 + 1/\gamma)^{1/2}$ [see Eq. (44a)], and therefore, when γ is large, the boundary-layer thickness is almost identical to that of the classical Cheng and Minkowycz (1977) boundary layer in which local thermal equilibrium is assumed. At smaller values of γ the boundary-layer thickness is greater, which indicates the increasing influence of the solid phase. We note that the ultimate boundary-layer thickness in terms of the original dimensional variable, $\bar{y}$, is

$$\bar{y} \propto \frac{\bar{x}^{1/2}\mu}{g\beta(T_w - T_\infty)K}\left[\frac{\varepsilon(1 + 1/\gamma)^{1/2}k_f^{1/2}}{\rho_f(\rho c)_f}\right] \quad (51)$$

The numerator of the term in square brackets in Eq. (51) is precisely $k_m^{1/2}$ where k_m, the effective conductivity of the saturated medium, is given by Eq. (3g).

The behavior of the fluid isotherms for very small values of γ is distinctive. Relatively near the leading edge the development of the fluid thermal field is unaffected by the large temperature difference between the phases; this is seen clearly in the isotherm plots for $\gamma = 10^{-5}$ and $\gamma = 10^{-4}$. Eventually the fluid thermal field thickens and local thermal equilibrium is achieved.

It is important to note that the solid phase isotherms do not terminate at some point on the y-axis at $x = 0$, as displayed in Fig. 2. Given the boundary-layer scalings, Eq. (4), the boundary-layer equations are valid as long as $x >> R^{-1}$, for otherwise $\hat{x}$ and $\hat{y}$ derivatives are formally of the same order of magnitude, and the boundary-layer approximation breaks down. A full treatment of the flow, for which these solid phase isotherms would be closed or join onto an insulated surface, would necessarily entail a solution of the full elliptic equations at points within an $O(R^{-1})$ distance of the origin. The present $x \to 0$ solutions would then be obtained as the near-leading-edge x-variable becomes large. This behavior has been confirmed in Rees (1998a).

Figures 3 and 4 display the evolution with ξ of the rates of surface heat transfer for both the solid and fluid phases for various values of γ. Figure 3 concentrates on those values of γ close to unity, while Fig. 4 is concerned with very small values of γ. In all cases the fluid rate of heat transfer decreases in magnitude as ξ increases, varying from b_0

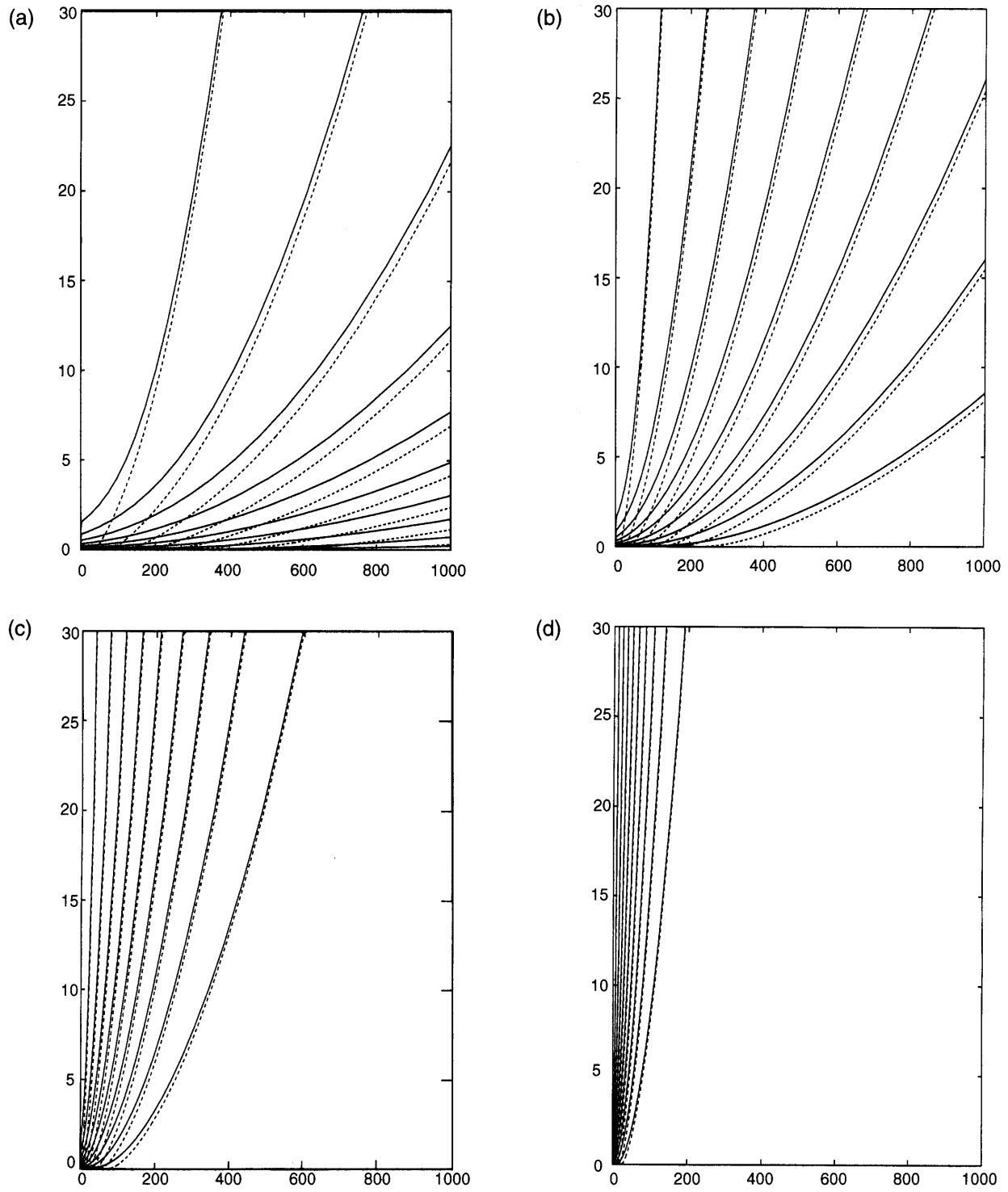

Figure 2. Isotherms for both the fluid phase (*solid lines*) and solid phase (*dashed lines*) for (a) $\gamma = 10^{-5}$, (b) 10^{-4}, (c) 10^{-3}, (d) 10^{-2}, (e) 10^{-1}, (f) 1, and (g) 10.

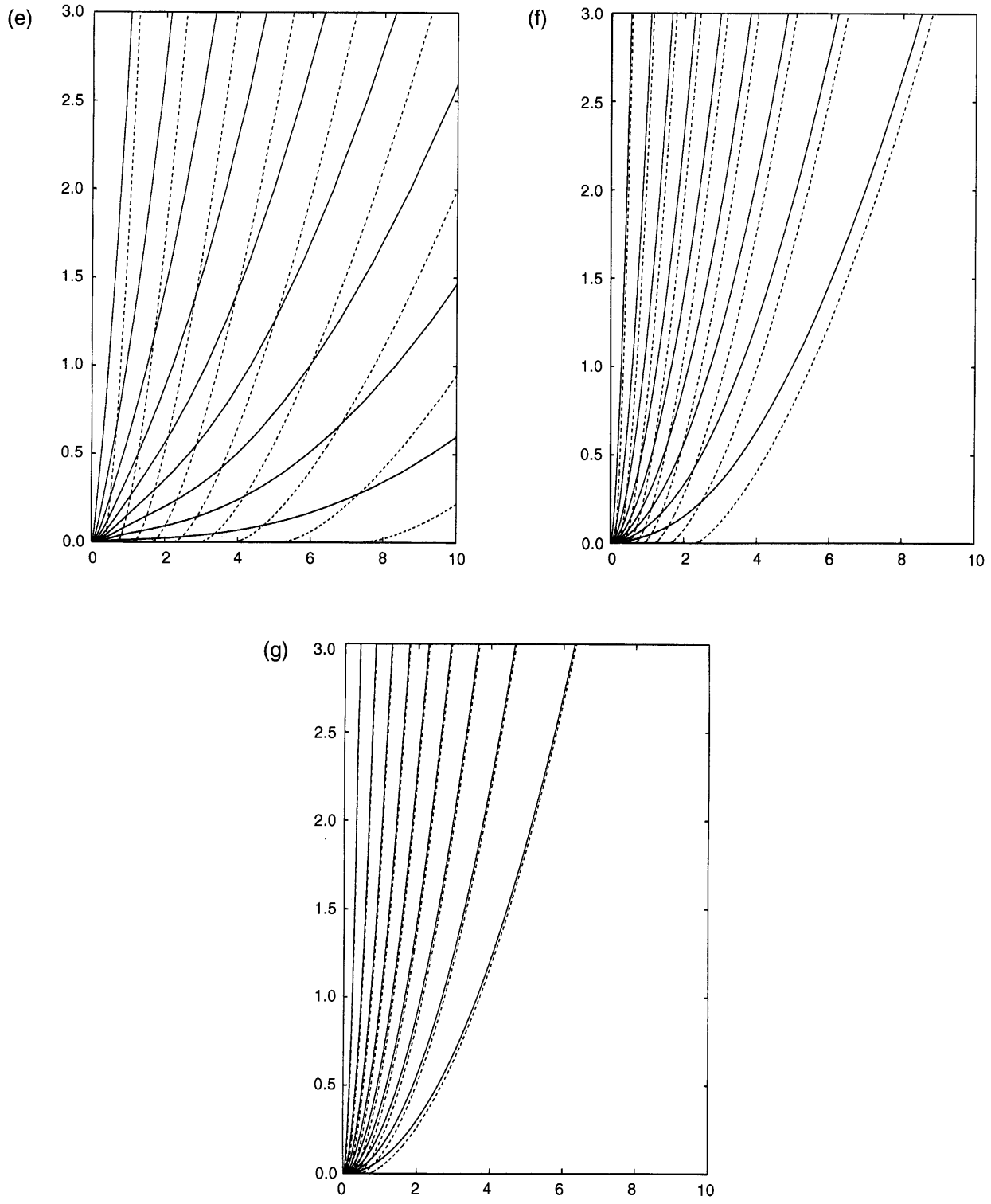

Figure 2. (*continued*)

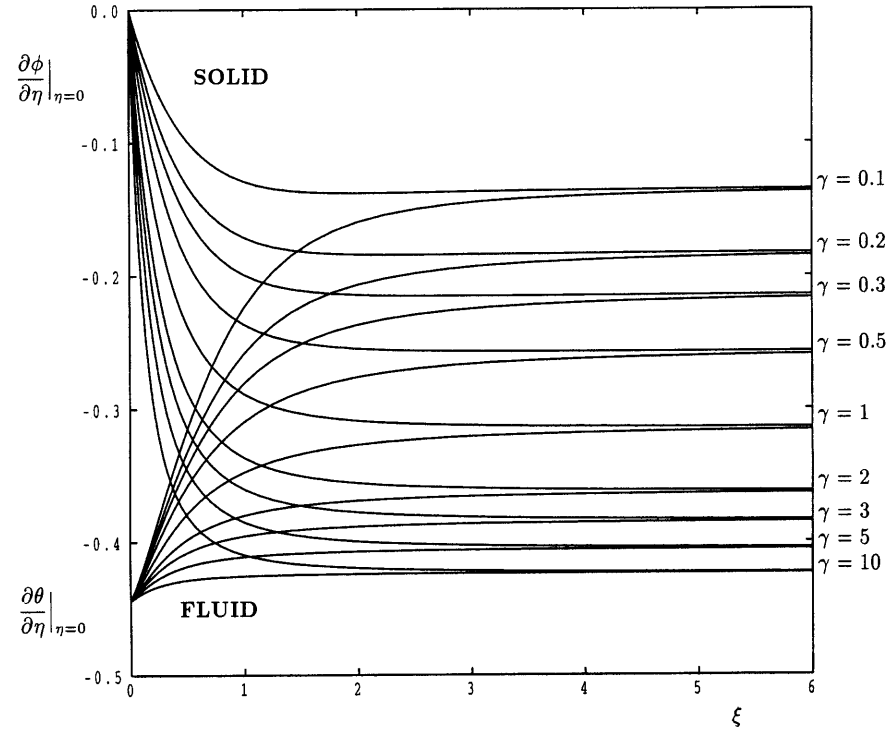

Figure 3. The evolution with ξ of the fluid and solid surface rates of heat transfer for various values of γ.

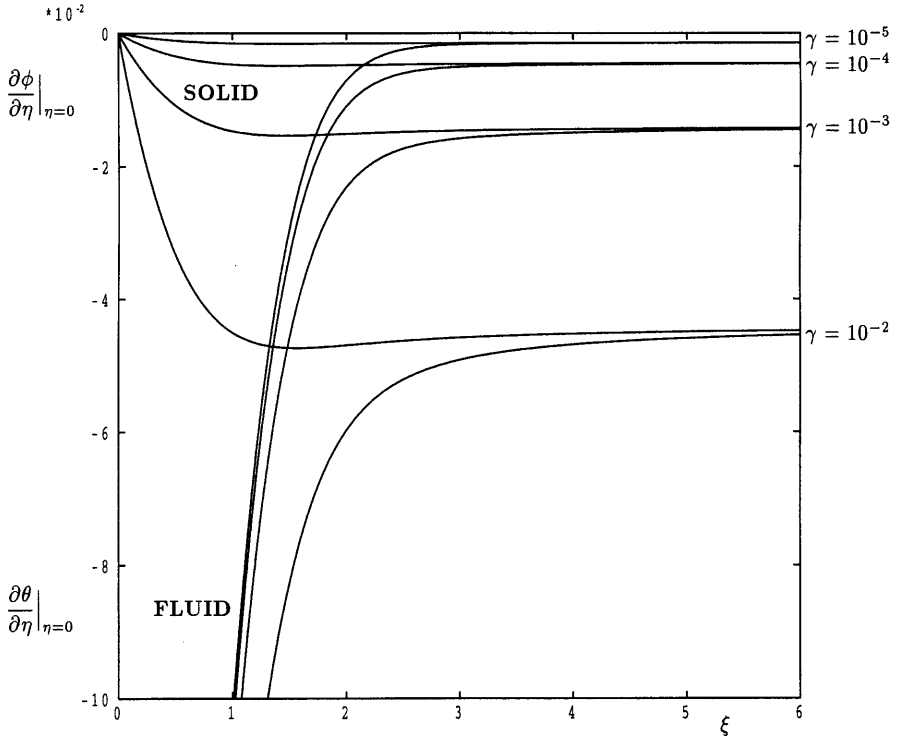

Figure 4. The evolution with ξ of the fluid and solid surface rates of heat transfer for various small values of γ.

at $\xi = 0$ to $b_0(1 + 1/\gamma)^{-1/2}$ as $\xi \to \infty$; see Eq. (50). Conversely, the solid rate of heat transfer increases in magnitude from zero until it becomes the same as that of the fluid phase.

In this article we have provided a necessarily detailed study of the effect of assuming a nonequilibrium model of thermal energy transport on the vertical thermal boundary-layer flow first examined by Cheng and Minkowycz (1977). The numerical simulation of the evolving nonsimilar boundary-layer flow is complicated considerably by the fact that the fluid and solid temperatures vary on asymptotically different length scales near the leading edge, and this information was used to formulate an appropriate numerical scheme. At large distances from the leading edge the flow attains local thermal equilibrium with the deviation from equilibrium being proportional to x^{-1} for large values of x.

ACKNOWLEDGMENT

The authors are grateful to the anonymous referees for their comments which improved the content and presentation of the paper.

REFERENCES

Amiri, A. and Vafai, K., Analysis of dispersion effects and non-thermal equilibrium, non-Darcian, variable porosity incompressible flow through porous media, *Int. J. Heat Mass Transfer,* vol. 37, pp. 939–954, 1994.

Cebeci, T. and Bradshaw, P., *Physical and Computational Aspects of Convective Heat Transfer,* Springer, New York, 1984.

Cheng, P. and Chang, I.-D., On buoyancy-induced flows in a saturated porous medium adjacent to horizontal heated surfaces, *Int. J. Heat Mass Transfer,* vol. 19, pp. 1267–1272, 1976.

Cheng, P. and Minkowycz, W. J., Free convection about a vertical flat plate embedded in a porous medium with application to heat transfer from a dike, *J. Geophys. Res.,* vol. 82, pp. 2040–2044, 1977.

Combarnous, M., Description du transfert de chaleur par convection naturelle dans une couche poreuse horizontale à l'aide d'un coefficient de transfert solide-fluide, *C. R. Acad. Sci. Paris,* vol. A275, pp. 1375–1378, 1972.

Combarnous, M. and Bories, S., Módelisation de la convection naturelle au sein d'une couche poreuse horizontal à l'aide d'un coefficient de transfert solide-fluid, *Int. J. Heat Mass Transfer,* vol. 17, pp. 505–515, 1974.

Daniels, P. G. and Simpkins, P. G., The flow induced by a heated vertical wall in a porous medium, *Q. J. Mech. Appl. Math.,* vol. 37, pp. 339–354, 1984.

Ingham, D. B. and Brown, S. N., Flow past a suddenly heated vertical plate in a porous medium, *Proc. R. Soc. Lond.,* Vol. A403, pp. 51–80, 1986.

Ingham, D. B. and Pop, I. (eds.), *Transport Phenomena in Porous Media,* Elsevier, Amsterdam, 1998, in press.

Kimura S., Kiwata, T., Okajima, A., and Pop, I. Conjugate natural convection in porous media, *Adv. Water Res.,* vol. 20, pp. 111–126, 1997.

Kuznetsov, A. V., A perturbation solution for nonthermal equilibrium fluid flow through a three-dimensional sensible heat storage packed bed, *Trans. ASME J. Heat Transfer,* vol. 118, pp. 508–510, 1996a.

Kuznetsov, A. V., Investigation of a non-thermal equilibrium flow of an incompressible fluid in a cylindrical tube filled with porous media, *J. Appl. Math. Phys. (ZAMP),* vol. 76, pp. 411–418, 1996b.

Kuznetsov, A. V., Analysis of a non-thermal equilibrium fluid flow in a concentric tube annulus filled with a porous medium, *Int. Commun. Heat Mass Transfer,* vol. 23, pp. 929–938, 1996c.

Kuznetsov, A. V., Thermal nonequilibrium forced convection in porous media, in *Transport Phenomena in Porous Media* (D. B. Ingham and I. Pop, eds.), Elsevier, Amsterdam, 1998.

Lage, J. L., The fundamental theory of flow through permeable media from Darcy to turbulence, in *Transport Phenomena in Porous Media* (D. B. Ingham and I. Pop, eds.), Elsevier, Amsterdam, 1998.

Lewis, S., Bassom, A. P., and Rees, D. A. S., The stability of vertical thermal boundary layer flow in a porous medium, *Eur. J. Mech. B: Fluids,* vol. 14, pp. 395–408, 1995.

Merkin, J. H. and Zhang, G., On the similarity solutions for free convection in a saturated porous medium adjacent to impermeable horizontal surfaces, *Warme Stoffubertr.,* vol. 25, pp. 179–184, 1990.

Merkin, J. H. and Zhang, G., The boundary-layer flow past a suddenly heated vertical surface in a saturated porous medium, *Warme Stoffubertr.,* vol. 27, pp. 299–304, 1992.

Nield, D. A. and Bejan, A., *Convection in Porous Media,* Springer, New York, 1992.

Rees, D. A. S., Nonlinear wave stability of vertical thermal boundary layer flow in a porous medium, *J. Appl. Math. Phys. (ZAMP),* vol. 44, pp. 306–313, 1993.

Rees, D. A. S., Three-dimensional free convection boundary layers in porous media induced by a heated surface with spanwise temperature variations, *Trans. ASME J. Heat Transfer,* vol. 119, pp. 792–798, 1997.

Rees, D. A. S., Vertical free convection boundary-layer flow in a porous medium using a thermal nonequilibrium model: elliptic effects, in *Proceedings of the Workshop on Applied Mathematics, Sylhet, Bangladesh, 1–3 September 1998,* 1998a.

Rees, D. A. S., Free convective boundary layer flow from a heated surface in a layered porous medium, *Journal of Porous Media,* 1998b, in press.

Rees, D. A. S. and Pop, I., Free convection induced by a horizontal wavy surface in a porous medium, *Fluid Dynam. Res.,* vol. 14, pp. 151–166, 1994.

Rees, D. A. S. and Bassom, A. P., The Blasius boundary layer

flow of a micropolar fluid, *Int. J. Engng. Sci.,* vol. 34, pp. 113–124, 1996.

Sözen, M. and Vafai, K., Analysis of the non-thermal equilibrium condensing flow of a gas through a packed bed, *Int. J. Heat Mass Transfer,* vol. 33, pp. 1247–1261, 1990.

Sözen, M., Vafai, K., and Kennedy, L. A., Thermal charging and discharging of sensible and latent heat storage packed beds, *J. Thermophys. Heat Transfer,* vol. 5, pp. 623–625, 1991.

Storesletten, L. and Rees, D. A. S., The influence of higher-order effects on the linear instability of thermal boundary layer flow in porous media, *Int. J. Heat Mass Transfer,* vol. 41, pp. 1833–1843, 1998.

Vafai, K. and Amiri, A., Non-Darcian effects in combined forced convective flows, in *Transport Phenomena in Porous Media* (D. B. Ingham and I. Pop, eds.), Elsevier, Amsterdam, 1998.